

Crystal Structure of a New Polymorph of $\text{Li}_2\text{FeSiO}_4$

Chutchamon Sirisopanorn,^{†,‡,¶} Adrien Boulineau,^{†,¶} Darko Hanzel,[‡] Robert Dominko,^{‡,¶} Bojan Budic,[‡]
A. Robert Armstrong,^{§,¶} Peter G. Bruce,^{§,¶} and Christian Masquelier^{*,†,¶}

[†]LRCS, Université de Picardie Jules Verne, 33 Rue Saint-Leu, 80039 Amiens, France, [‡]National Institute of Chemistry, Hajdrihova 19, SI-1000 Ljubljana, Slovenia, [‡]Institute Jozef Stefan, Jamova 39, SI-1000 Ljubljana, Slovenia, [§]EaStCHEM, School of Chemistry, University of St. Andrews, St. Andrews, Fife KY16 9ST, U.K., and [¶]ALISTORE-ERI, 80039 Amiens Cedex, France

Received April 17, 2010

We report on the crystal structure of a new polymorph of $\text{Li}_2\text{FeSiO}_4$ (prepared by annealing under argon at 900 °C and quenching to 25 °C) characterized by electron microscopy and powder X-ray and neutron diffraction. The crystal structure of $\text{Li}_2\text{FeSiO}_4$ quenched from 900 °C is isostructural with $\text{Li}_2\text{CdSiO}_4$, described in the space group $Pmnb$ with lattice parameters $a = 6.2836(1)$ Å, $b = 10.6572(1)$ Å, and $c = 5.0386(1)$ Å. A close comparison is made with the structure of $\text{Li}_2\text{FeSiO}_4$ quenched from 700 °C, published recently by Nishimura et al. (*J. Am. Chem. Soc.* 2008, 130, 13212). The two polymorphs differ mainly on the respective orientations and alternate sequences of corner-sharing FeO_4 and SiO_4 tetrahedra.

1. Introduction

Lithium transition-metal silicates with the general formula Li_2MSiO_4 ($M = \text{Fe}, \text{Mn}, \text{Co}$) have recently attracted research interest since the introduction of $\text{Li}_2\text{FeSiO}_4$ as a potential positive electrode material in lithium batteries in 2001.¹ The incorporation of $(\text{SiO}_4)^{4-}$ polyanions (strong Si–O bonds) in the crystal structure is anticipated, as in LiFePO_4 ,² to result in enhanced electrochemical and chemical stability.³ The theoretical capacity of ca. 160 mAh g^{-1} , corresponding to 1 Li^+ extracted per Li_2MSiO_4 , and the abundance of raw materials (particularly true for Fe and Si) have enhanced their potential to become cathode materials of choice for large-scale battery applications. Additionally, the possibility of extracting up to two Li^+ per Li_2MSiO_4 (i.e., operating on both $\text{M}^{2+}/\text{M}^{3+}$ and $\text{M}^{3+}/\text{M}^{4+}$ redox couples), especially for manganese,^{4,5} would lead to a major breakthrough and is definitely worth a detailed investigation. Recently, the low intrinsic conductivity of $\text{Li}_2\text{FeSiO}_4$ has been overcome not only by carbon coating but also by lowering of the particle size, resulting in a satisfactory performance in terms of capacity and cycle life.^{4,5}

These results have highlighted the potential of $\text{Li}_2\text{FeSiO}_4$ or even higher operating voltage materials, $\text{Li}_2\text{Fe}_{1-x}\text{Mn}_x\text{SiO}_4$, as new positive electrode materials.

Even though there have been substantial recent improvements in the electrochemical performance of these silicates, the crystal chemistry of $\text{Li}_2\text{FeSiO}_4$ remains ambiguous because of a combination of the rich polymorphism exhibited by this material and hence the difficulties encountered in obtaining single-phase samples. Several recent publications have described $\text{Li}_2\text{FeSiO}_4$, obtained from different synthetic routes, as being isostructural with $\beta\text{-Li}_3\text{PO}_4$, i.e., crystallizing in the orthorhombic space group $Pmn2_1$ with lattice parameters $a = 6.27$ Å, $b = 5.33$ Å, and $c = 5.01$ Å.^{6–11} As mentioned by Quoirin et al.^{12,13} and by Nishimura et al.,¹⁴ the indexation given by Nyten et al.³ was probably questionable, and further work needed to be done to clarify the crystal structures of $\text{Li}_2\text{FeSiO}_4$. Quoirin et al.^{12,13} reported the existence

*To whom correspondence should be addressed. E-mail: christian.masquelier@u-picardie.fr.

(1) Armand, M.; Michot, C.; Ravet, N.; Simoneau, M.; Hovington, P. European patent EP 1 134 826 A1, 2001.

(2) Padhi, A. K.; Nanjundaswamy, K. S.; Goodenough, J. B. *J. Electrochem. Soc.* 1997, 144, 1188.

(3) Nyten, A.; Abouimrane, A.; Armand, M.; Gustafsson, T.; Thomas, J. O. *Electrochem. Commun.* 2005, 7, 156.

(4) Dominko, R.; Bele, M.; Gaberscek, M.; Meden, A.; Remskar, M.; Jamnik, J. *Electrochem. Commun.* 2006, 8, 217.

(5) Gong, Z. L.; Li, Y. S.; He, G. N.; Li, J.; Yang, Y. *Electrochem. Solid State Lett.* 2008, 11, A60.

(6) Tarte, P.; Cahay, R. C. R. *Hebd. Seances Acad. Sci.* 1970, C271, 777.

(7) O'Keeffe, M.; Hyde, B. G. *Acta Crystallogr.* 1978, B34, 3519.

(8) Zaghbi, K.; Ait Salah, A.; Ravet, N.; Mauger, A.; Gendron, F.; Julien, C. M. *J. Power Sources* 2006, 160, 1381.

(9) Li, L. M.; Guo, H. J.; Li, X. H.; Wang, Z. X.; Peng, W. J.; Xiang, K. X.; Cao, X. *J. Power Sources* 2009, 1, 45.

(10) Peng, Z. D.; Cao, Y. B.; Hu, G. R.; Du, K.; Gao, X. G.; Xiao, Z. W. *J. Power Sources* 2009, 1, 45.

(11) Dompablo, M. E.; Gallardo-Amores, J. M.; Garcia-Martinez, J.; Morán, E.; Tarascon, J.-M.; Armand, M. *Solid State Ionics* 2008, 179, 1758.

(12) Quoirin, G.; Taulelle, F.; Dupont L.; Masquelier, C. 211th ECS Meeting, 2007; Abstract 98.

(13) Quoirin, G. Ph.D. Thesis, Université de Picardie Jules Verne, Amiens, France, 2007. Quoirin, G.; Tarascon, J. M.; Masquelier, C.; Delacourt, C.; Poizat, P.; Taulelle, F. World Patent WO2008/107571 A2, 2008.

(14) Nishimura, S.; Hayase, S.; Kanno, R.; Yashima, M.; Nakayama, N.; Yamada, A. *J. Am. Chem. Soc.* 2008, 130, 13212.

Table 1. Reported Structural Data on $\text{Li}_2\text{FeSiO}_4$ in the Literature

sample	a (Å)	b (Å)	c (Å)	β (deg)	space group
LFS@100	6.2652(1)	10.8121(1)	4.9504(1)		$Pbn2_1$ ¹³
LFS@400	6.2709(8)	5.3382(7)	4.9651(7)		$Pnm2_1$ ¹³
LFS@800	8.2278(1)	5.0204(6)	8.2295(1)	99.231(4)	$P2_1$ ^{a,14}
LFS@700	8.2253(5)	5.0220(1)	8.2381(4)	99.230(2)	$P2_1/n$ ¹⁵
LFS@750	6.270(4)	5.331(1)	5.022(1)		$Pnm2_1$ ³
LFS@800	10.664(1)	12.540(2)	5.022(1)		$Cmma$ ^{12,13}
LFS@900	6.2853(5)	10.6592(8)	5.0367(4)		$Pmnb$ [this work]
LFS@900	6.2835(7)	10.6572(1)	5.0386(5)	89.941(4)	$P2_1/n$ [this work]

^a Communicated orally by Yamada et al., during the LiBd (Lithium Battery Discussion) meeting held in Arcachon (France) in Sept 2009, to be more reliably described in the $P2_1/n$ space group

of several polymorphs for $\text{Li}_2\text{FeSiO}_4$ depending on the annealing temperature: $\text{Li}_2\text{FeSiO}_4$ was proposed at that time to crystallize at 800 °C in the $Cmma$ space group with $a = 10.66$ Å, $b = 12.54$ Å, and $c = 5.02$ Å and at 900 °C in the $Pmnb$ space group (isostructural with $\text{Li}_2\text{CdSiO}_4$) with $a = 6.28$ Å, $b = 10.66$ Å, and $c = 5.04$ Å. Recently, Nishimura et al.¹⁴ determined the structure of $\text{Li}_2\text{FeSiO}_4$ (synthesized from a ceramic-type route at 800 °C) in the $P2_1$ space group (corrected orally by the authors to $P2_1/n$ in Sept 2009) with $a = 8.23$ Å, $b = 5.02$ Å, $c = 8.23$ Å, and $\beta = 99.20^\circ$, and we subsequently proposed indexation in the $P2_1/n$ space group.¹⁵ A summary of attributed space groups and unit-cell parameters of different $\text{Li}_2\text{FeSiO}_4$ polymorphs is given in Table 1.

The proposed structural models for $\text{Li}_2\text{FeSiO}_4$ are derived from Li_3PO_4 -based structures, in which half of the tetrahedral sites, generated by a distorted hexagonal close packing of oxygen atoms, are occupied by cations. Li_3PO_4 itself crystallizes in two main groups of polymorphs (β and γ), which differ in the respective orientations of the filled tetrahedra: all T^+ (oriented upward) in the low-temperature β form and T^+ and T^- (oriented downward) for the high-temperature γ form.^{16,17} In even more complicated systems (three types of cations, for instance), the structures of Li_2MSiO_4 analogues ($\text{M} = \text{Zn}, \text{Mn}, \text{Mg}, \text{Co}$) have been reported to adopt “simple” β - or γ -type structures or their distorted derivatives.^{18–22}

In this work, we report on the crystal structure of a new polymorph of $\text{Li}_2\text{FeSiO}_4$ (prepared by annealing under argon at 900 °C and quenching to 25 °C) characterized by electron microscopy and powder X-ray and neutron diffraction. We present inductively coupled plasma atomic emission spectroscopy (ICP-AES) analysis and Mössbauer spectroscopy data for this new polymorph.

2. Experimental Section

2.1. Synthesis. The new polymorph of $\text{Li}_2\text{FeSiO}_4$ (labeled as LFS@900) was synthesized by a solid-state reaction between Li_2SiO_3 (Aldrich), “FeO” (Aldrich), and Fe^0 (Riedel de Haen), with the latter of these being used to compensate for the slight nonstoichiometry of Fe_{1-x}O . The precursors were mixed using a high-energy ball mill, SPEX 8000 M Mixer/Mill, for 1 h prior to

transferring to a stainless steel tube and sealed under an argon atmosphere. Thereafter, the starting mixture was heated to 900 °C for 7 days and subsequently quenched to 25 °C.

2.2. Characterization. The Li:Fe:Si ratio of the obtained sample was determined using an ICP optical emission spectrometer (Varian 715-ES) equipped with Sturman–Master spray chamber and a V-groove nebulizer. Prior to the analysis, 20 mg of each sample was dissolved in a few drops of concentrated HCl and the obtained solution was diluted up to 100 mL volume. The measurement uncertainty, which includes accuracy and reproducibility, was lower than 3% in this set of experiments.

The oxidation number of iron, its local environments, and the purity of the obtained products were analyzed by ⁵⁷Fe Mossbauer experiments. The measurements were performed at 298 K. The source was ⁵⁷Co in a rhodium matrix. Velocity calibration and isomer shifts were quoted relative to an absorber of metallic iron at room temperature. The experiments were performed in transmission geometry. Parameter fits were performed using a standard least-squares fitting routine with Lorentzian lines.

The X-ray diffraction (XRD) patterns of the $\text{Li}_2\text{FeSiO}_4$ samples were collected at 298 K using a Bruker D8 powder diffractometer in Bragg–Brentano θ – θ geometry with the $\text{Cu K}\alpha$ radiation. The machine was equipped with a LinxEye detector that allows energy discrimination (to remove part of the fluorescence). The data were recorded in the 2θ range 10–90° with a step size of $\approx 0.02^\circ$ (2θ) and a constant counting time of 12 s per step. The patterns were analyzed by full pattern matching and/or Rietveld refinement as implemented in the *Fullprof* program.²³ The first step of the structure determination was made ab initio using the *FOX* program.²⁴

Time-of-flight powder neutron diffraction data were obtained on the Polaris high-intensity, medium-resolution instrument at ISIS at the Rutherford Appleton Laboratory. Because lithium is a neutron absorber, the data were corrected for absorption. The final structural model was refined by the Rietveld method using the program TOPAS Academic.²⁵

Electron diffraction patterns were recorded using a FEI TECNAI F20 S-TWIN transmission electron microscope at an accelerating voltage of 200 kV and equipped with a double-tilt specimen holder. The powders were dispersed in acetonitrile, and droplets of these suspensions were then deposited on lacey-carbon grids inside a glovebox. In order to protect the crystallites from air exposure ($\text{Li}_2\text{FeSiO}_4$ may be slightly sensitive to air, depending on the relative humidity and on the particle size), grids were set on the holder inside the glovebox and the holder was transferred to the microscope using a homemade device. Electron diffraction experiments were carried out on many crystallites, and reproducible results were observed. Particles studied were chosen as isolated as possible and as thin as possible. Great care was taken to use an incident beam as soft as possible. Patterns were

(15) Boulineau, A.; Sirisopanaporn, C.; Dominko, R.; Armstrong, A. R.; Bruce, P. G.; Masquelier, C. *Dalton Trans.* **2010**, DOI: 10.1039/c002815k.

(16) West, A. R.; Glasser, F. P. *J. Solid State Chem.* **1972**, *4*, 20.

(17) Frayret, C.; Masquelier, C.; Villesuzanne, A.; Morcrette, M.; Tarascon, J. M. *Chem. Mater.* **2009**, *21*, 1861.

(18) Yamaguchi, H.; Akatsuka, K. *Acta Crystallogr.* **1979**, *B35*, 2678.

(19) Iskhakova, L. D.; Rybakov, V. B. *Crystallogr. Rep.* **2003**, *48*, 44.

(20) Politaev, V. V.; Petrenko, A. A.; Nalbandyan, V. B.; Medvedev, B. S.; Shvetsova, E. S. *J. Solid State Chem.* **2007**, *180*, 1045.

(21) Yamaguchi, H.; Akatsuka, K. *Acta Crystallogr.* **1979**, *B35*, 2680.

(22) Lyness, C.; Delobel, B.; Armstrong, A. R.; Bruce, P. G. *Chem. Commun.* **2007**, 4890 and references cited therein.

(23) Carvajal, J. R. See also a report in CPD of IUCr, Newsletter 26, 2001, 12; available at <http://www.iucr.org/iucr-top/comm/cpd/Newsletters>, 1993, 55.

(24) Favre-Nicolin, V.; Cerny, R. *J. Appl. Crystallogr.* **2002**, *35*, 734.

(25) Coelho, A. A. *J. Appl. Crystallogr.* **2000**, *33*, 899.

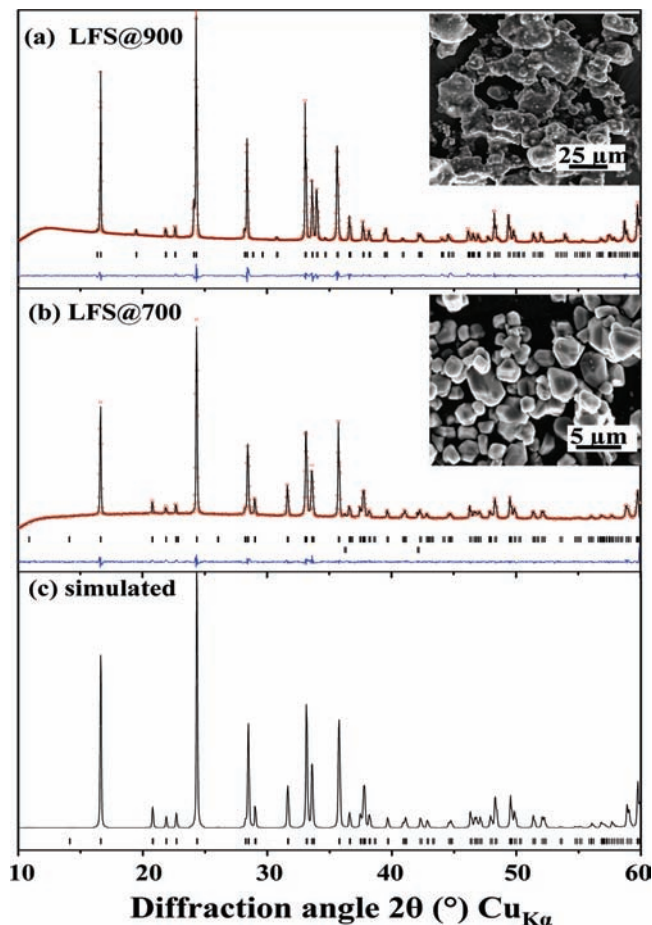


Figure 1. XRD patterns (recorded with Cu K α radiation) of two polymorphs of Li₂FeSiO₄: LFS@900 (a); LFS@700 (b). Part b corresponds to the structure published by Nishimura et al.,¹⁴ and its simulated pattern in *P2₁/n* is given in part c.

successively collected by tilting the grids around a given direction; the preserved state of the crystallites studied was checked by tilting back the grids and verifying the agreement of the patterns with the previous ones. High-resolution images could not be recorded because of the need for a very intense beam, which would damage the material.

3. Results and Discussion

As observed by the XRD patterns and scanning electron microscopy micrographs shown in Figure 1a (insets), the LFS@900 sample consists of well-crystallized particles. Owing to the high-temperature treatment, particles were strongly sintered and exhibited very large shape and size distributions, ranging from a few micrometers to 100 μ m in size. The XRD pattern of the LFS@900 grayish-white powder shows significant differences in the Bragg positions and intensities in comparison with that of the same composition annealed at 700 °C (LFS@900)^{12,14} (Figure 1b,c).

The obtained powder was further characterized by means of ICP and Mossbauer spectroscopy. The Li:Fe:Si ratio was found to be 2.02:1.1:1, i.e., close to the expected stoichiometric values, given that traces of crystallized Fe_{1-x}O were found to coexist with Li₂FeSiO₄. Figure 2 shows the Mossbauer spectrum and the fitted parameters. The spectrum of LFS@900 was fitted as being composed of two doublets: the main one from Li₂FeSiO₄ (Fe²⁺) itself and the second one from traces [3.6(2) atom %] of nonstoichiometric

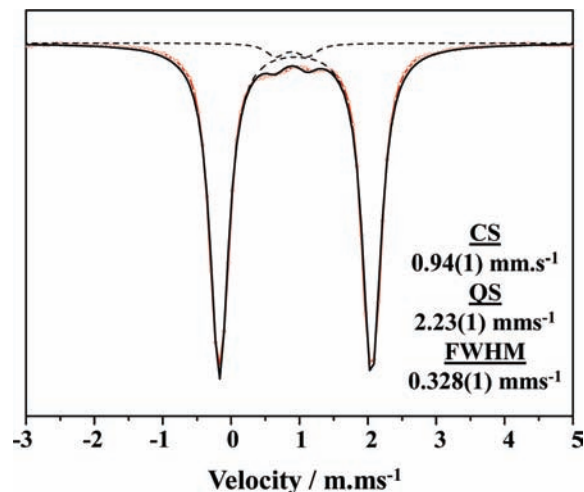


Figure 2. Mossbauer spectrum of LFS@900.

Fe_{1-x}O (Fe²⁺ and Fe³⁺).²⁶ The values of centroid shifts (CSs) and quadrupole splitting (QS) gathered for the new polymorph of Li₂FeSiO₄ investigated here are within the usual ranges observed for tetrahedrally coordinated Fe⁽²⁺⁾ in glasses and/or crystallized compositions.^{27,28}

Figure 3 presents four electron diffraction patterns collected from the same crystal successively tilted around a common direction as marked by the arrows. The reciprocal space could be reconstructed in the projection along the tilt direction. The reconstruction involving replacement of all of these patterns in a two-dimensional space (see Figure 3b) gives rise to an orthorhombic cell with parameters of ≈ 6.2 and ≈ 10.6 Å in direct space. The third parameter is linked to the direction around which the crystal was tilted, the common direction, and is evaluated as ≈ 5 Å. The patterns were fully indexed after reconstruction with the parameters of the new unit cell depicted in Figure 3. The approximate lattice constants of LFS@900 observed by transmission electron microscopy images are in close correspondence with those of γ_{II} -Li₂MSiO₄ where M = Zn, Mg, Mn, and Cd.^{18,19,29,30} Although some of the γ_{II} structures have been reported to crystallize in the monoclinic system with space group *P2₁/n*, others, such as Li₂CdSiO₄,²⁹ were reported with an orthorhombic unit cell in the space group *Pmnb*.

In order to check the validity of the lattice parameters extracted from electron diffraction, refinements of XRD data were carried out in the profile fitting mode using the space group *P1* (triclinic) with fixed values of $\alpha = \gamma = 90^\circ$. The three cell parameters and β angle were refined, the last of these to check for the presence of a monoclinic distortion. The refined lattice parameters were $a = 6.2819(1)$ Å, $b = 10.6575(2)$ Å, and $c = 5.0371(1)$ Å. The β angle was found to be $90.032(7)^\circ$. Such a small departure from 90° is far beyond the resolution of electron diffraction as well as that of "standard" powder XRD. At this stage of the crystallographic investigation, both orthorhombic and monoclinic (very small β angle) systems were considered as plausible solutions for the cell description. On the basis of an examination of the systematic

(26) Greenwood, N. N.; Howe, A. T. *Dalton Trans.* **1972**, 6, 110.

(27) Darby Dyar, M. *Am. Mineral.* **1985**, 70, 304.

(28) Nyten, A.; Kamali, S.; Haggstrom, L.; Gustafssona, T.; Thomas, J. O. *J. Mater. Chem.* **2006**, 16, 2266.

(29) Riekel, C. *Acta Crystallogr.* **1977**, B33, 2656.

(30) Yu, S. C.; Smith, D. K.; Austerman, S. B. *Am. Mineral.* **1978**, 63, 1241.

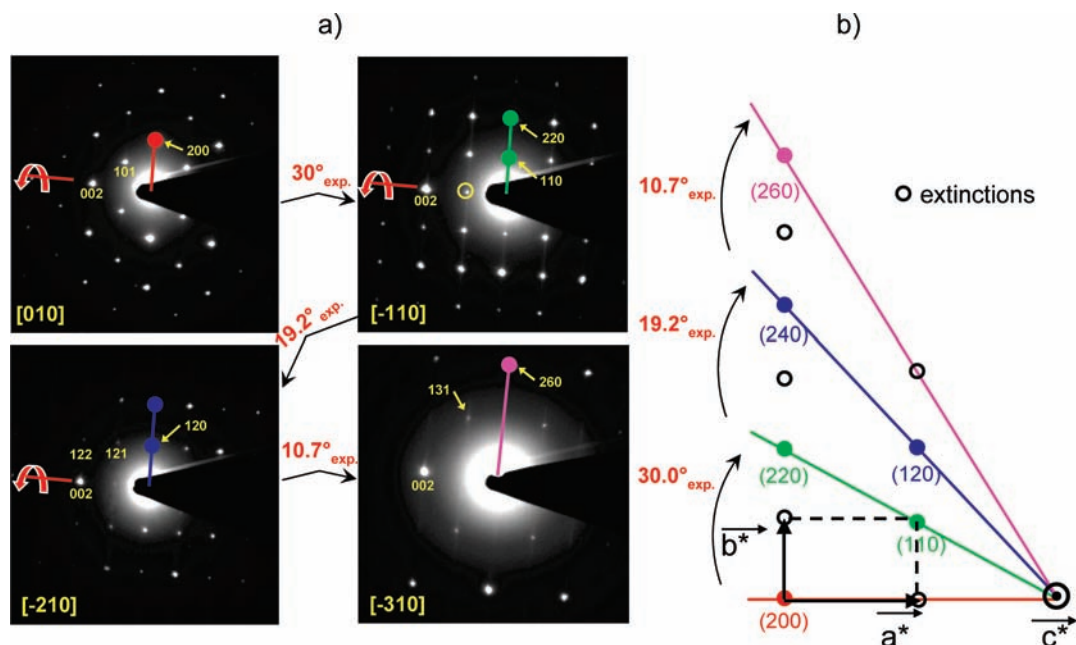


Figure 3. Four electron diffraction patterns of LFS@900 obtained by rotation around a common direction (a) and the corresponding indexation (b).

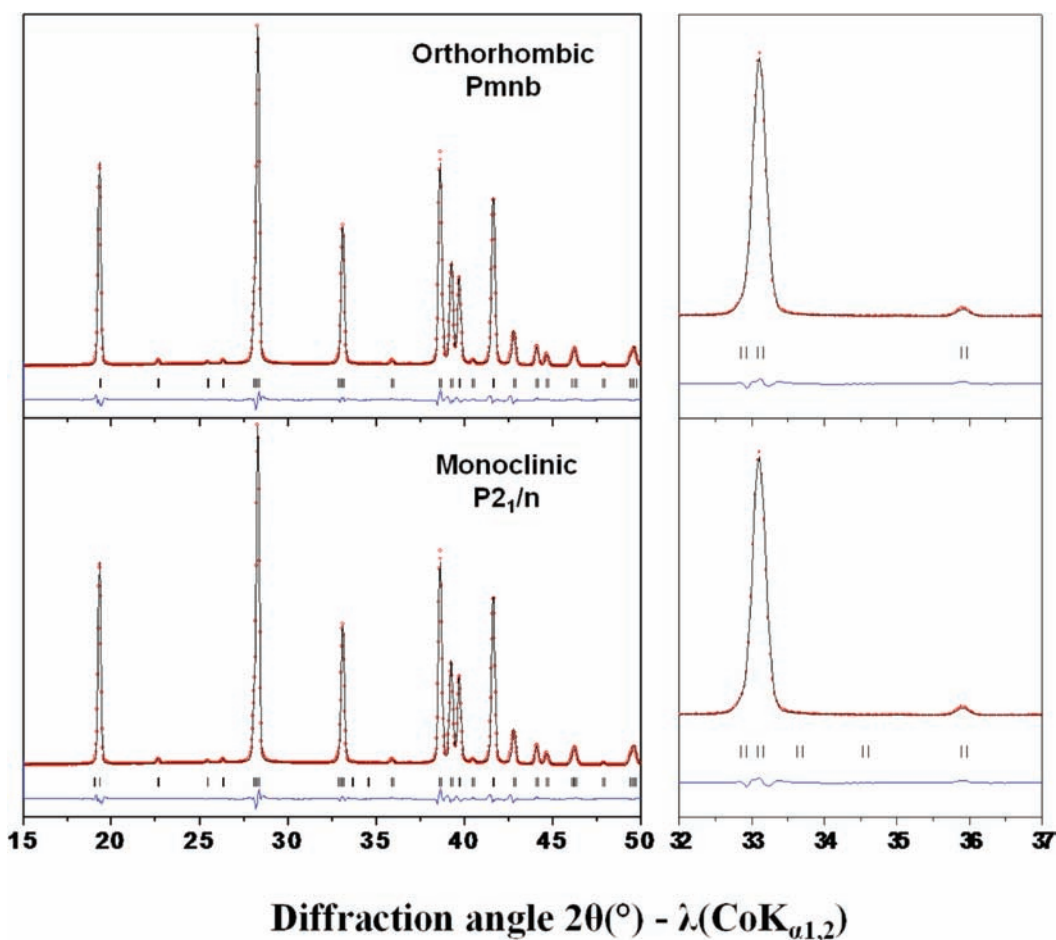


Figure 4. Enlarged zones of XRD patterns (recorded with Co K α radiation) of LFS@900 indexed in the two possible space groups $Pmnb$ and $P2_1/n$ with their respective Bragg positions. Note that the fit appears to be excellent in both cases.

absences in both XRD and electron diffraction patterns, the $P2_1/n$ (monoclinic) and $Pmnb$ (orthorhombic) space groups were chosen with the unit cell parameter values given in

Table 1. These refined cell parameters of LFS@900 are similar to those of the γ structures (high-temperature forms) for Li_2MSiO_4 materials ($M = \text{Zn, Mg, Mn, Cd}$) described in

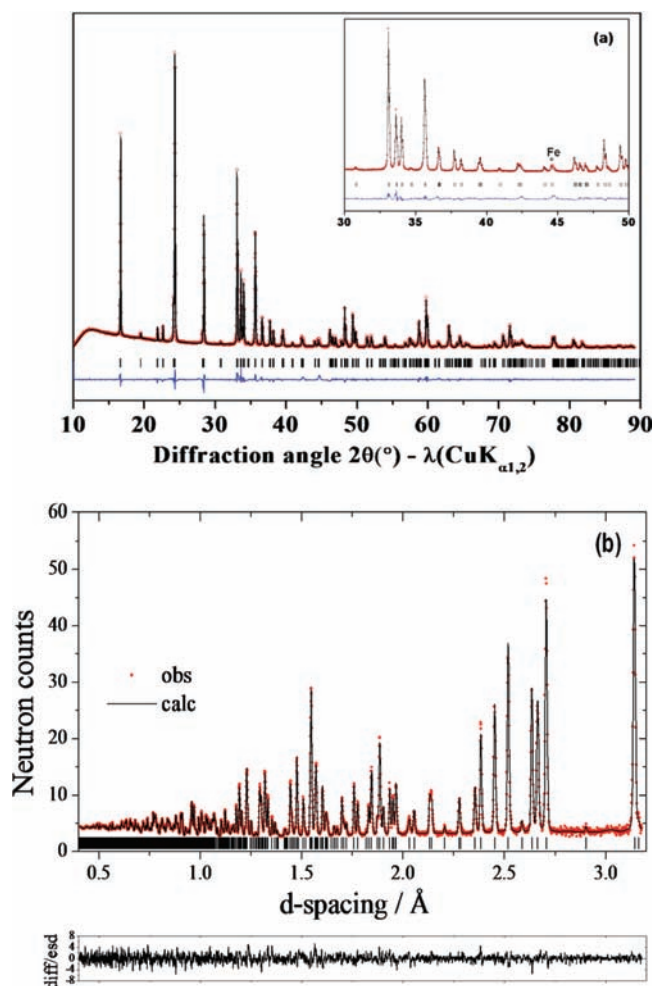


Figure 5. Rietveld refinements in the $Pnmb$ space group of the crystal structure of LFS@900 from XRD (a) and neutron diffraction (b) data.

the $P2_1/n$ and/or $Pnmb$ space groups. To the best of our knowledge, the crystal structure of isostructural $\text{Li}_2\text{FeSiO}_4$ has never been reported.

Full-pattern-matching refinements of XRD data gave very good reliability factors for both space groups: $R_p = 6.2\%$, $R_{wp} = 7.9\%$, and $\chi^2 = 86.6$ for $Pnmb$; $R_p = 5.8\%$, $R_{wp} = 7.4\%$, and $\chi^2 = 75.0$ for $P2_1/n$, as illustrated in Figure 4. From these considerations only, the (very slight) monoclinic distortion appears plausible, but one should point out that the Bragg positions generated by both space groups are poorly distinguishable, except in the $33.5 < 2\theta_{\text{Co K}\alpha} < 35.0$ region. The absence of any diffracted intensity in this region did not permit one, hence, to attribute with certainty the space group $P2_1/n$ to LFS@900, and we decided to adopt the $Pnmb$ space group for the full structure determination, described below.

The crystal structure of the new LFS@900 phase was first solved ab initio by the global optimization of a structural model in direct space using simulated annealing (in parallel tempering mode), as implemented in the recently developed program FOX.²⁴ The initial structure model was then refined using the Rietveld method, and Fourier difference maps were used to check the accord between the electron density distribution and integrated intensities observed in the experimental pattern. The powder neutron diffraction pattern was refined in space group $Pnmb$ using as starting coordinates those of $\text{Li}_2\text{CdSiO}_4$.²⁹ Fe_{1-x}O was added as a second phase.

Table 2. Atomic Coordinates, Occupancies, and Atomic Displacement Parameters Obtained by Rietveld Refinement of Time-of-Flight Powder Neutron Diffraction Data for $\text{Li}_2\text{FeSiO}_4$ (LFS@900) in Space Group $Pnmb$ ^a

site	Wyckoff	occupancy	x	y	z	$B/\text{\AA}^2$
Li1	8d	1	0.0044(4)	0.3302(3)	0.2163(6)	1.05(3)
Fe1	4c	1	0.25	0.58133(6)	0.2016(2)	0.687(9)
Si1	4c	1	0.25	0.4164(1)	0.6970(3)	0.34(1)
O1	4c	1	0.25	0.4107(1)	0.3710(2)	0.62(1)
O2	4c	1	0.25	0.5631(1)	0.7809(3)	0.57(1)
O3	8d	1	0.0384(1)	0.34383(6)	0.8055(2)	0.535(8)

^a $Pnmb$; $a = 6.28377(7)$ \AA, $b = 10.6573(1)$ \AA, $c = 5.0385(1)$ \AA, $R_{wp} = 1.71\%$, $R_p = 2.91\%$, $R_c = 1.28\%$.

Table 3. Selected Bond Lengths (\AA) and Angles (deg) of $\text{Li}_2\text{FeSiO}_4$ (LFS@900)^a

	O1	O2	O3	O3
(a) FeO_4				
O1	2.006(2)	110.16(6)	111.81(3)	111.81(3)
O2	3.389(9)	2.127(2)	91.09(4)	91.09(4)
O3	3.303(5)	2.935(1)	1.983(8)	132.44(6)
O3	3.303(5)	2.935(1)	3.628(7)	1.983(8)
(b) SiO_4				
O1	1.647(3)	106.76(1)	108.65(8)	108.65(8)
O2	2.626(2)	1.625(2)	111.70(7)	111.70(7)
O3	2.660(1)	2.692(1)	1.628(1)	109.28(1)
O3	2.660(1)	2.692(1)	2.655(1)	1.628(1)
(c) LiO_4				
O1	1.917(3)	113.73(2)	116.53(1)	107.04(1)
O2	3.244(6)	1.958(3)	115.60(1)	92.97(1)
O3	3.282(3)	3.300(1)	1.942(3)	107.64(1)
O3	3.221(7)	2.935(1)	3.254(2)	2.088(3)

^a The numbers in the boldface diagonals are M–O distances (M = Fe, Si, Li). The numbers below the boldface diagonals are O–O distances. The numbers above the boldface diagonals are O–M–O angles.

Possible Li/Fe disorder was investigated using each model but gave no improvement to the fit.

Refined (using the Rietveld method) powder XRD and neutron diffraction patterns are given in parts a and b of Figure 5, respectively. The atomic coordinates and reliability factors obtained for the two proposed solutions are listed in Table 2, and the very low values of the final R_{wp} and R_p reveal the quality of the proposed solutions. This is further supported by the very consistent list of interatomic distances and angles given in Table 3 for the $Pnmb$ description.

The refined structure consists of a distorted buckled hexagonal close-packed array of oxygen layers stacked perpendicularly to the orthorhombic c axis, between which cations occupy half of the tetrahedral sites. Between oxygen “layers”, each cationic “slab” is built from a succession of $\text{FeO}_4/\text{SiO}_4$ and LiO_4 chains running along [100] (Figure 6). Within each type of chain, FeO_4 and SiO_4 tetrahedra alternate in opposite directions, while all LiO_4 tetrahedra are pointing in the same direction. Figure 6 illustrates clearly the main structural differences between this new LFS@900 structure and that of LFS@700 proposed by Nishimura et al.¹⁴ While the $\cdots\text{Fe}-\text{Si}-\text{Fe}-\text{Si}-\text{Fe}\cdots$ sequence is common to both structures (along $[10-1]_{\text{LFS@700}}$ equal to $[100]_{\text{LFS@900}}$), the respective orientations of FeO_4 and SiO_4 tetrahedra along $[010]_{\text{LFS@700}} = [001]_{\text{LFS@900}}$ are different: up–up–down–down–up–up–down–down for LFS@700 up–down–up–down–up–down–up–down–up–down for LFS@900. The comparison

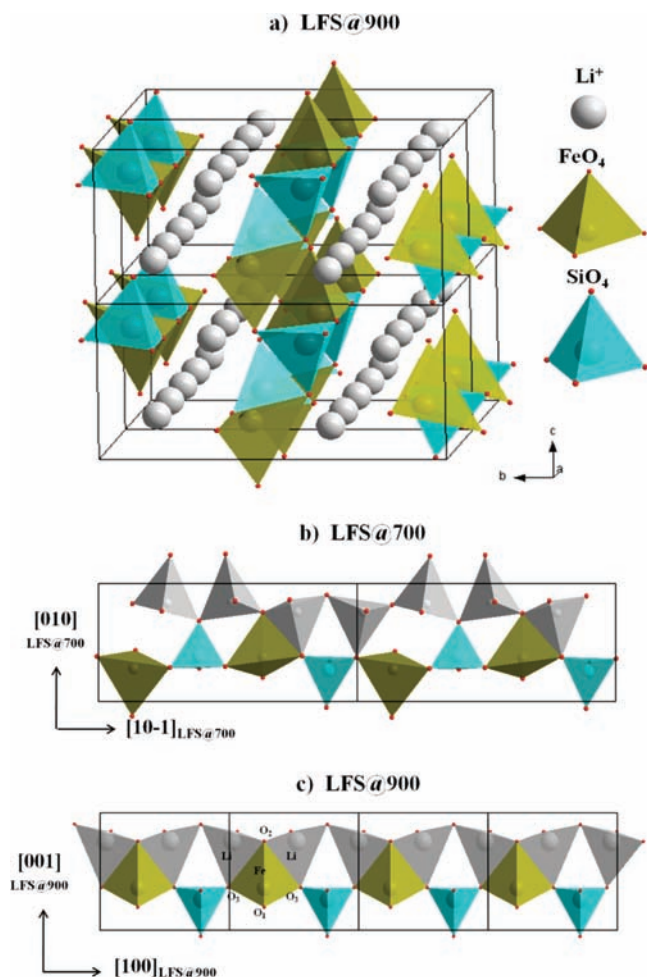


Figure 6. (a) Representation of the crystal structure of LFS@900 and (b and c) comparisons of the tetrahedral orientations along equivalent directions in LFS@700¹⁴ and LFS@900.

between both structures is further described in Figure 7, which also gives the corresponding relationships between the unit cells.

Along the [001]_{LFS@900} direction, layers are linked through common corners and edge sharing between LiO₄ and FeO₄. Note that FeO₄ and SiO₄ tetrahedra never have common edges because of (i) the big difference between Fe–O and Si–O bond lengths and (ii) larger Fe²⁺–Si⁴⁺ repulsions in comparison to Li⁺–Fe²⁺. Regarding the structural model itself, SiO₄ tetrahedra are quite regular, whereas FeO₄ and the two LiO₄ tetrahedra are much more distorted (Table 3). Typical Si–O, Fe–O, and Li–O distances are 1.66, 2.03, and 1.96 Å, respectively. They are in very good agreement with the interatomic distances predicted from the ionic radii for Si⁴⁺, Fe⁴⁺, and Li⁺ tetrahedrally coordinated by O²⁻, i.e., 1.64, 2.01, and 1.97 Å, respectively.³¹ The FeO₄ and LiO₄ distortions can be explained by the fact that they share common edges.

(31) Shannon, R. D.; Prewitt, C. T. *Acta Crystallogr.* **1969**, B25, 925.

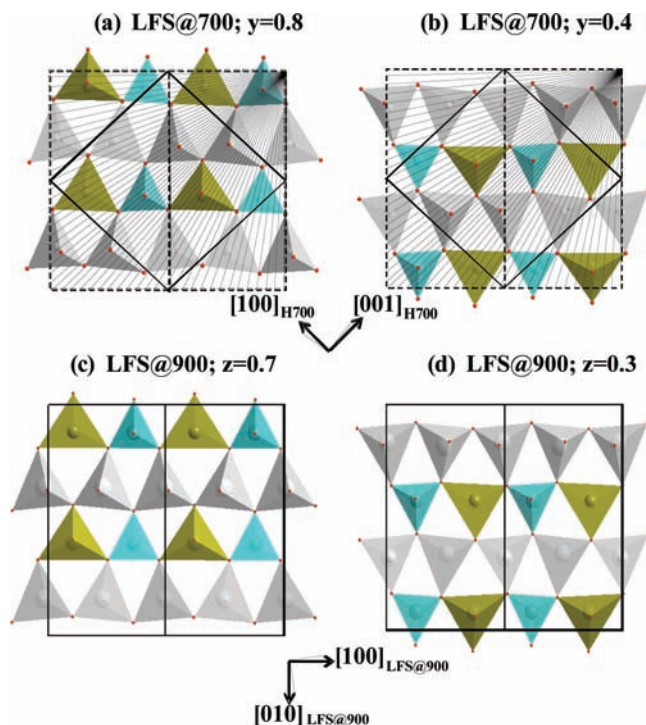


Figure 7. Further comparisons of tetrahedral arrangements between LFS@700 and LFS@900.

4. Conclusion

We have found and described here the crystal structure of a new polymorph for Li₂FeSiO₄, quenched from 900 °C, thanks to precise complementary studies through electron microscopy, XRD, and neutron diffraction. It is isostructural with Li₂CdSiO₄, described in the space group *Pm̄nb*, with lattice parameters $a = 6.2836(1)$ Å, $b = 10.6572(1)$ Å, and $c = 5.0386(1)$ Å. It differs from the structure recently published by Nishimura et al. (quenched from 800 °C¹⁴) by the respective orientations and alternating sequences of corner-sharing FeO₄ and SiO₄ tetrahedra.

This study offers an interesting basis for the study of the electrochemical properties of such a composition. In close connection with the density functional theory calculations underway¹⁷ and precise electrochemical measurements/titrations, we investigate how the kinetics (rate at which Li⁺ can be extracted/inserted) and thermodynamics (equilibrium potential for the Fe³⁺/Fe²⁺ redox couple) of this material would be affected.

Acknowledgment. We thank G. Quoirin, F. Taulelle, and M. Casas Cabanas, with whom this work had been initiated, and L. Dupont and J. M. Tarascon for discussion. The Ministère de l'Enseignement Supérieur et de la Recherche, France, is acknowledged for supporting C.S. through an international Ph.D. student scholarship shared between Amiens (France) and Ljubljana (Slovenia).